Journal of Alloys and Compounds 584 (2014) 327–330

Contents lists available at ScienceDirect

Journal of Alloys and Compounds

journal homepage: www.elsevier.com/locate/jalcom

Investigation and impact of oxygen plasma compositions on cubic ZnMgO grown by Molecular Beam Epitaxy

R. Casey Boutwell [a], M. Wei [a], Matthieu Baudelet [b], Winston V. Schoenfeld [a,*]

[a] CREOL, The College of Optics & Photonics, University of Central Florida, Orlando, FL, United States
[b] Townes Laser Institute, CREOL, The College of Optics & Photonics, University of Central Florida, Orlando, FL, United States

ARTICLE INFO

Article history:
Received 4 June 2013
Received in revised form 11 August 2013
Accepted 11 September 2013
Available online 20 September 2013

Keywords:
Oxygen plasma
Cubic ZnMgO
Optical emission spectroscopy

ABSTRACT

ZnMgO thin films were grown by Molecular Beam Epitaxy on closely-lattice-matched MgO substrates with a Radio-Frequency (RF) generated oxygen plasma. The impact on the cubic ZnMgO of oxygen flow rate and applied RF power was investigated under a high vacuum condition (1E-6 Torr). Optical Emission Spectroscopy identified active species in the plasma including O, O^+, and O_2^+. The emission intensity of these species was compared at oxygen flow rates ranging from 0.5 sccm to 2.5 sccm and applied RF powers from 150 W to 500 W. Plasma composition at operating conditions was determined by correlating changes in optical emission to changes in relative concentration of active species in the plasma. Atomic Force Microscopy and profilometry characterized changes in surface roughness and growth rate of produced films. Independently increasing flow rate and RF power increased growth rate while simultaneously decreasing roughness. Growth rate enhancement of 80% was achieved with an improvement in surface roughness from 7.5 nm to 3.3 nm in a 1 μm square. Optimal conditions are discussed for ZnMgO thin film epitaxy.

1. Introduction

ZnMgO thin films attract considerable attention due to the ability to tune optical absorption from the near ultraviolet (NUV) to the deep ultraviolet (DUV) by varying metallic composition [1,2]. DUV optoelectronics can access the solar blind spectral region, enabling commercial applications ranging from combustion monitors and DUV detectors to UV sterilization equipment. While it is well known that the binaries ZnO and MgO have incompatible crystal structures, Zn-rich ZnMgO (wurtzite B4) and Mg-rich ZnMgO (rocksalt B1) are regularly produced with good crystallinity and smooth surface morphology at different ends of the compositional scale [3,4]. Adding Mg to the ZnO lattice blueshifts the ternary bandgap, while redshifting is accomplished by adding Zn to MgO [5,6].

While wurtzite-ZnMgO has received significant attention for its functionality in the NUV spectral range [7,8], cubic-ZnMgO has recently also begun to receive attention from several research groups. c-ZnMgO possesses many intriguing characteristics worthy of investigation and exploitation by optoelectronic devices and is readily grown on commercially available MgO substrates, and maintains good crystallinity with epilayer roughnesses at the angstrom level [1]. Additionally, c-ZnMgO is inversion symmetric, enabling isotropic conduction of charge carriers and avoiding the polarization fields present in wurtzite phase quantum-confined structures. Devices with internal polarization fields like those present in wurtzite can suffer from reduced electron–hole overlap similar to the Quantum Confined Stark Effect [9,10].

While epitaxial ZnMgO thin films are produced by many techniques [11–14], plasma-enhanced Molecular Beam Epitaxy (MBE) offers fine control over process environment by utilizing a Radio-Frequency (RF) oxygen plasma source. Oxygen plasma injection entails a number of unique variables and criteria, including system stability and reproducibility by avoiding oxidation of internal components or reduction of elemental flux through source oxidation [15]. These considerations act as boundary conditions on oxygen flow into the growth reactor and applied power to the injected plasma. Active species in the oxygen plasma must also be considered for their ability to etch and react with substrates and internal machinery, often requiring the use of high voltage deflection plates or electrostatic ion traps at the source aperture to redirect harmful reactive ions and improve net growth rate by reducing film etching [16,17].

Previous investigations considered the effect of oxygen plasma factors in ZnO, but a thorough study of the impact of oxygen plasma conditions in c-ZnMgO has not been reported [18,19]. Here we investigate the effect of oxygen flow rate and applied RF power on the growth rate and surface morphology of c-ZnMgO thin films grown on MgO substrates.

* Corresponding author.
E-mail address: winston@creol.ucf.edu (W.V. Schoenfeld).

0925-8388/$ - see front matter © 2013 Published by Elsevier B.V.
http://dx.doi.org/10.1016/j.jallcom.2013.09.064

2. Experimental details

The ZnMgO films were grown in an SVT Associates oxide MBE reactor on 1 cm square (1 0 0) MgO substrates purchased from MTI Crystal. Praxair Ultra High Purity (99.9999%) oxygen was injected through a mass flow controller at a flow rate of 0.5–2.5 sccm in 0.5 sccm steps into the SVT 4.5ALO plasma source. An RF generator operating at 13.56 MHz was coupled to the source and supplied powers at 50 W increments between 150 W and 500 W. The ignited plasma was stabilized for 60 min before Optical Emission Spectroscopy (OES) was collected by an Ocean Optics Jaz fiber-coupled spectrometer. The optical fiber was affixed outside a sapphire window on the plasma source and aimed axially down the inductively-coupled plasma tube. Each subsequent spectrum was collected after 10 min stabilization at new operating conditions. Films were grown at substrate temperature of 275 °C, with fixed Mg and Zn cell temperatures (345 °C and 360 °C respectively) for a total of 4 h of growth per film. The Zn crucible operated with an aperture to reduce source oxidation, while the Mg crucible was operated without an aperture. The plasma source was operated without the use of deflection plates (electrostatic ion traps) which resulted in all species in the plasma impinging on the surface during growth. All substrates were outgassed in a separate ultra-high vacuum chamber for 4 h at 750 °C. The growth chamber base pressure was below 1E-9 Torr and growth pressure ranged from 1E-8 Torr at 0.5 sccm flow rate to 1E-5 Torr at 2.5 sccm.

ZnMgO thin films were investigated with a number of characterization tools. A Vecco Dimension 3100 Atomic Force Microscope (AFM) measured surface morphology while standard contact profilometry measured film thickness and allowed for determination of the film growth rate. A Rigaku D-max X-ray Diffractometer (XRD) searched for phase segregation in the produced films, while a Cary 500 UV–Vis Spectrophotometer investigated absorption edge with changing oxygen flow rate and applied RF power.

Spectral peaks were identified from the NIST Atomic Spectra Database [20]. Three active species were detected in the oxygen plasma: neutrally charged atomic oxygen (O I), singly ionized atomic oxygen (O II), and singly ionized molecular oxygen (O_2^+, the dioxygenyl ion). Excited neutral atomic oxygen (O I) was measured from changes in the 6453 Å line, excited singly-ionized atomic oxygen (O II) was identified by the 4367 Å line, and changes in excited ionized molecular oxygen (O_2^+) were identified by the vibronic transition at 5248 Å. The assumption that changes in emission intensity related directly to changes in plasma composition was applied to correlate the relative concentrations of these active species. This allowed for the determination of relative maxima and minima in the ratio of neutral atomic to ionized atomic oxygen and neutral atomic to ionized molecular oxygen by identifying maxima in the ratio of their emission intensities.

3. Results and discussion

Fig. 1 shows a spectra collected from optical emission along the axis of the plasma source. The spectrum contains many transitions, but describes only the three active species. The O I spectrum is strongest at the 777 nm and 844 nm unresolved triplets, representing transitions from $3p^5P–3s^5S$ and $3p^3P–3s^3S$ lines respectively. O II emission is brightest from the 436 nm peak representing combined emission from transitions between $3p^4P–3s^4P$ and $3d^2D–3p^2D$. O_2^+ emission is evident as broad peaks between 500 nm and 650 nm representing the first negative O_2^+ system [21]. The spectrometer used did not resolve the fine structure spin components of these separate transitions, resulting in their appearance as a single emission line. Due to the saturation of the O I spectrum at 777 nm and 844 nm, the unresolved 615 nm triplet for O I corresponding to a $4d^5D–3p^5P$ was chosen to represent changes in O I concentration instead.

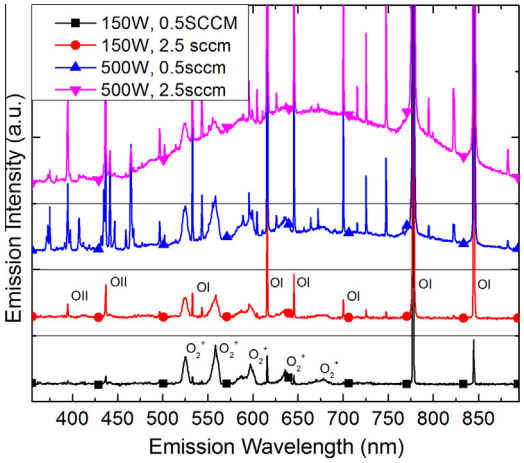

Fig. 1. Typical emission spectra of oxygen plasma under extremes of flow and power shows the broad emission of Bremsstrahlung radiation, which is maximized at highest flow and power. The low power curves show strong contribution from molecular oxygen emission, while higher power resulted in strong emission from oxygen atoms.

Increasing the power and flow rate through the plasma source increased the intensity of the emission lines. At high flow, a broad increase in intensity was observed between 450 nm and 900 nm resulting from Bremsstrahlung radiation emission. This general brightening at high flow covered the emission of a number of spectral lines. At low flow and low power the number of spectral lines was dramatically reduced, and resulted in higher relative intensity of broad molecular emission peaks than atomic lines as seen in Fig. 1.

The change in intensity was compared between O I, O II, and O_2^+ to determine relative changes in concentration of active species in the plasma. Fig. 2 shows the ratios O I/O II and O I/O_2^+ as functions of flow rate and RF power. It is interesting to note that the graph shows two maxima to optimize the difference between the neutral atoms and the more reactive atomic ions; at 1.5 sccm and 350 W, and at around 2.5 sccm 350 W. The first maximum at 1.5 sccm may be preferred for growth due to the reduced likelihood of source oxidation at lower oxygen flux.

To investigate whether this is caused by increasing atomic concentration or decreasing molecular concentration, Fig. 2b has been

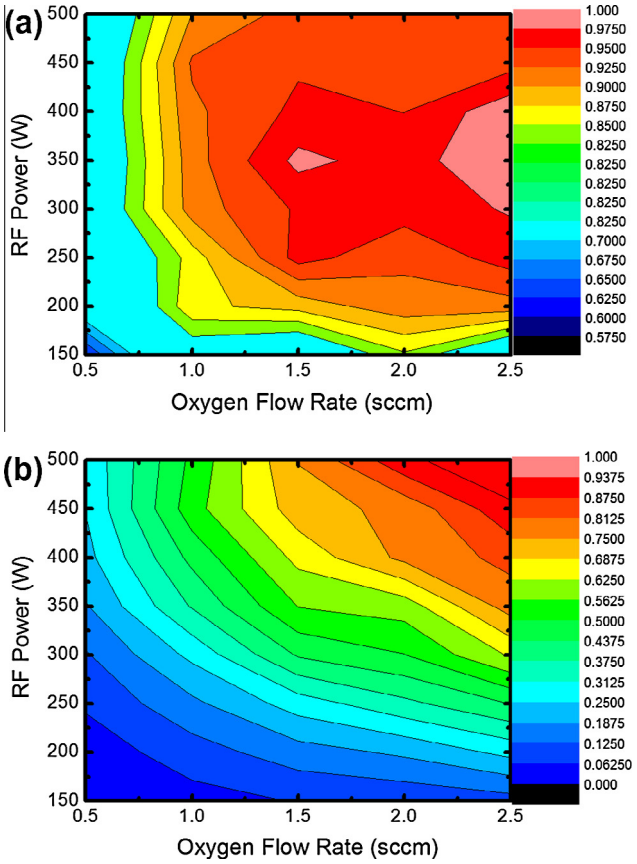

Fig. 2. (a) The emission intensity ratios of neutral (OI) to ionized (OII) atomic oxygen shows the first relative maximum at 1.5 sccm and 350 W. Similar conditions exist at higher flow, but may lead to source oxidation and reduced metal flux and (b) emission intensity ratio of neutral atomic oxygen (OI) to ionized molecular oxygen (O_2^+) showing a monotonic increase with RF power and oxygen flow.

decoupled and is shown in Fig. 3. Fig. 3a is the normalized absolute intensity of O I measured by OES, while Fig. 3b is the normalized absolute intensity of O_2^+. Fig. 3a confirms that as power and oxygen flow rate increase the atomic concentration of the plasma increases monotonically. However, contrary to the case of molecular emission of nitrogen in GaN growth, where emission intensity increases with power and flow [22], here the molecular emission intensity decreases with increasing power and flow. Fig. 3b shows a peak concentration of ionized oxygen molecules at 0.5 sccm and 250 W applied RF power. This difference can be explained by their difference in dissociation energies (6.66 eV for O_2^+ and 9.76 eV for N_2) if the molecules were formed from ions/neutrals, as well as a lower ionization potential for O_2 (12.08 eV) than N_2 (15.58 eV) if the molecular ions were formed by ionization. These parameters can explain the existence of neutral N_2 in a larger range of low pressure and low temperature than O_2^+.

Independently increasing the oxygen flow rate and the applied RF power resulted in increased growth rate and decreased surface roughness of produced ZnMgO films. Increased Zn incorporation was also evident in both cases from optical transmission. However, in the case of increasing plasma power, it was found that increased Zn incorporation may lead to phase segregation when grown near the miscibility gap. The films produced demonstrated optical bandgaps decreasing from 5.4 eV to 5.2 eV with increasing plasma power. Fig. 4 shows the impact of changing RF power on ZnMgO film growth rate and 1 μm RMS roughness. As power is increased, the concentration of atomic oxygen rises and allows for greater Zn incorporation, thus increasing the growth rate (solid line). Increased Zn binding results in smoother film surfaces until the incorporation efficiency pushes the film into phase segregation. Segregation occurred at 400 W and 500 W and resulted in a dramatic increase in film roughness (dotted line).

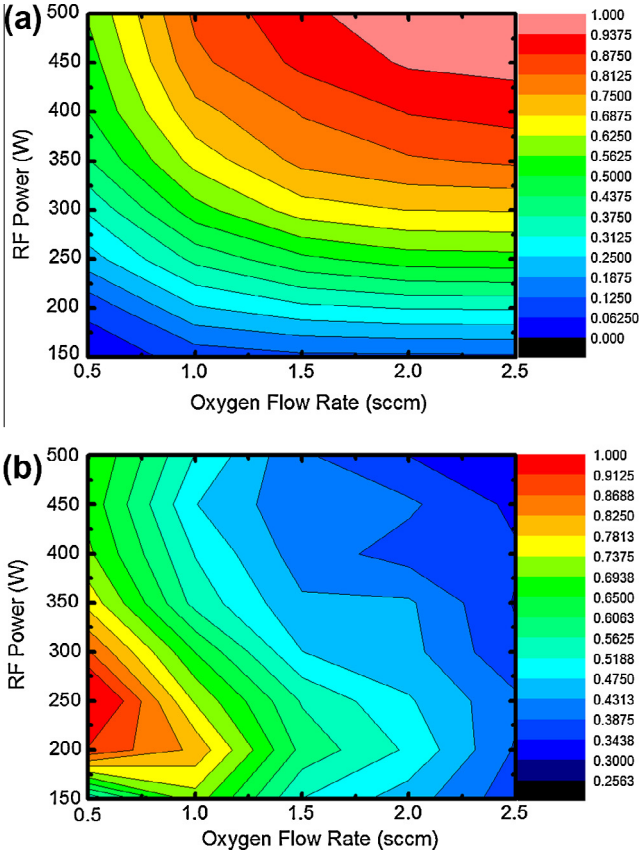

Fig. 3. (a) Normalized emission intensity of neutral atomic oxygen (O I) showing monotonic increase and (b) normalized emission intensity of ionized molecular oxygen (O_2^+) showing relative maximum at low oxygen flow and low RF power.

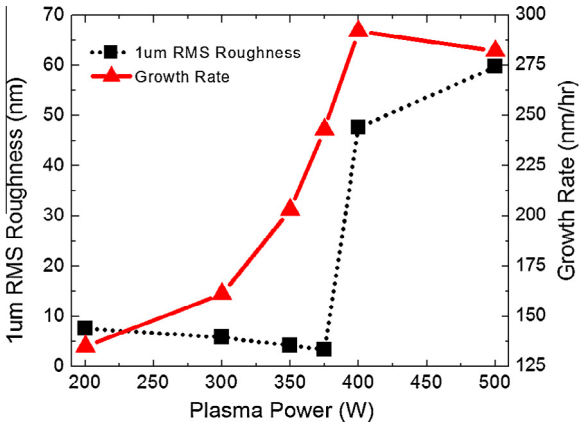

Fig. 4. Increasing oxygen plasma power resulted in increased growth rate. 1 μm AFM scans showed decreasing roughness until phase segregation began at 400 W.

Increased Zn incorporation with increasing atomic oxygen can be understood by considering the enthalpy of formation (ΔH) for MgO and ZnO. ΔH is nearly twice as high for MgO as it is for ZnO (601 kJ/mol compared to 348 kJ/mol), indicating that at similar surface concentration, MgO formation is energetically favorable. With little available atomic oxygen to bind with in the low flow, low RF power scenario, Mg accumulates a disproportionate amount of the oxygen on the surface. However, as the atomic oxygen concentration increases (with increasing flow or with increasing RF power), Zn incorporation efficiency is correspondingly increased, allowing for better ZnMgO formation and smoother films. Additional discussion and impact of this behavior on solar-blind ultraviolet sensors is published elsewhere [23].

4. Conclusion

Increased oxygen flow rate and RF power were found to result in increased growth rate and reduced roughness. The OI/O_2^+ ratio increased monotonically with both flow and power, but the O I/O II ratio was found to exhibit a peak at 1.5 sccm and 350 W RF applied power. This suggests that for smooth ZnMgO films the main damaging reactive species is O_2^+ not O II, and that it is more important to minimize O_2^+ than to maximize the difference between O I and O II. Alternatively, a higher concentration of O_2^+ is beneficial for films with more textured surfaces.

These results show that smooth ZnMgO films with relatively high growth rate may be produced at the high end of the oxygen flow (2.5 sccm) and RF power (500 W) investigated. However, as hardware and cation source oxidation is a constant threat, these results indicate that the preferred condition is at 500 W, 1.5 sccm, where decreased oxygen flow will reduce reactor oxidation and maximize growth campaign duration.

Further investigation with additional *in situ* equipment may enable more direct connections between O I, O II, and O_2^+ concentrations and their effect on epilayer growth and microstructure evolution. One possible technique to understand these physics more deeply is to operate the oxygen source with deflection plates and a quadrupole mass spectrometer to select active species with a set mass/charge ratio. In this scenario O I, O II, and O_2^+ could be individually selected and directed at the substrate during growth to determine the empirical impact of oxidation with these three different species.

Acknowledgments

The authors acknowledge the financial support of the U.S. Army Research Office under Contract No. W911NF-10-1-0159, monitored by Dr. Michael Gerhold.

References

[1] J.W. Mares, R.C. Boutwell, A. Scheurer, W.V. Schoenfeld, J. Mater. Res. 25 (2010) 1072–1079.
[2] Y.N. Hou, Z.X. Mei, Z.L. Liu, T.C. Zhang, X.L. Du, Appl. Phys. Lett. 98 (2011).
[3] L.K. Wang, Z.G. Ju, C.X. Shan, J. Zheng, B.H. Li, Z.Z. Zhang, B. Yao, D.X. Zhao, D.Z. Shen, J.Y. Zhang, J. Cryst. Growth 312 (2010) 875–877.
[4] S. Sadofev, S. Blumstengel, J. Cui, J. Puls, S. Rogaschewski, P. Schafer, Y.G. Sadofyev, F. Henneberger, Appl. Phys. Lett. 87 (2005).
[5] M. Wei, R.C. Boutwell, J.W. Mares, A. Scheurer, W.V. Schoenfeld, Appl. Phys. Lett. 98 (2011).
[6] W. Yang, S.S. Hullavarad, B. Nagaraj, I. Takeuchi, R.P. Sharma, T. Venkatesan, R.D. Vispute, H. Shen, Appl. Phys. Lett. 82 (2003) 3424–3426.
[7] T. Gruber, C. Kirchner, R. Kling, F. Reuss, A. Waag, Appl. Phys. Lett. 84 (2004) 5359–5361.
[8] H. Zhu, C.X. Shan, L.K. Wang, J. Zheng, J.Y. Zhang, B. Yao, D.Z. Shen, J. Phys. Chem. C 114 (2010) 7169–7172.
[9] F. Bernardini, V. Fiorentini, D. Vanderbilt, Phys. Rev. B 56 (1997) 10024–10027.
[10] B. Monemar, G. Pozina, Prog. Quantum Electron. 24 (2000) 239–290.
[11] W.I. Park, G.C. Yi, H.M. Jang, Appl. Phys. Lett. 79 (2001) 2022–2024.
[12] J.W. Kim, H.S. Kang, J.H. Kim, S.Y. Lee, J.K. Lee, M. Nastasi, J. Appl. Phys. 100 (2006).
[13] Y.M. Zhao, J.Y. Zhang, D.Y. Jiang, C.X. Shan, Z.Z. Zhang, B. Yao, D.X. Zhao, D.Z. Shen, ACS Appl. Mater. Interfaces 1 (2009) 2428–2430.
[14] J. Liang, H.Z. Wu, Y.F. Lao, D.J. Qiu, N.B. Chen, T.N. Xu, Chin. Phys. Lett. 21 (2004) 1135–1138.
[15] Y.S. Kim, N. Bansal, S. Oh, J. Vac. Sci. Technol. A 28 (2010) 600–602.
[16] M. Wei, R.C. Boutwell, G.A. Garrett, K. Goodman, P. Rotella, M. Wraback, W.V. Schoenfeld, J. Alloys Comp. 552 (2013) 127–130.
[17] T.L. Goodrich, Z. Cai, M.D. Losego, J.P. Maria, K.S. Ziemer, J. Vac. Sci. Technol. B 25 (2007) 1033–1038.
[18] W.C.T. Lee, P. Miller, R.J. Reeves, S.M. Durbin, J. Vac. Sci. Technol. B 24 (2006) 1514–1518.
[19] K. Sakurai, M. Kanehiro, K. Nakahara, T. Tanabe, S. Fujita, S. Fujita, J. Cryst. Growth 209 (2000) 522–525.
[20] Y.R. Alexander Kramida, Joseph Reader, Natl. Inst. Stands. Technol. (2013).
[21] M. Tuszewski, J.T. Scheuer, J.A. Tobin, J. Vac. Sci. Technol. A 13 (1995) 839–842.
[22] E. Iliopoulos, A. Adikimenakis, E. Dimakis, K. Tsagaraki, G. Konstantinidis, A. Georgakilas, J. Cryst. Growth 278 (2005) 426–430.
[23] R.C. Boutwell, M. Wei, W.V. Schoenfeld, Appl. Phys. Lett. 103 (2013) 031114.